

## The Kinetics of DNA–Cationic Vesicle Complex Formation

P. C. A. Barreleiro\* and B. Lindman

Center for Chemistry and Chemical Engineering, Physical Chemistry 1, University of Lund,  
P.O. Box 124, 221 00 Lund, Sweden

Received: December 13, 2002

Stopped-flow fluorescence studies were performed to investigate the kinetics of formation of complexes between DNA and cationic vesicles. We followed the kinetics as a function of charge ratio and lipid vesicle composition. Binary mixtures of a saturated cationic lipid, dioctadecyldimethylammonium bromide (DODAB), and a zwitterionic lipid, dioleoylphosphatidylethanolamine (DOPE), were used to prepare small unilamellar vesicles at 25 °C. The binding followed first-order reactions and occurred stepwise. The results presented indicate the existence of a three-step mechanism for cationic vesicle “binding” to DNA: first DNA rapidly adsorbs onto the oppositely charged membrane surface (milliseconds), and thereafter, on a longer time scale (seconds), the formed DNA–lipid complex continues to aggregate and grow; a third step is also observed, which seems to be due to rearrangement of the complex with a further change of the DNA conformation. The time constant of each step was determined by the relative amounts of DNA and cationic vesicles and the composition of the lipid bilayer of the vesicles.

### Introduction

Cationic vesicles appear as promising gene delivery vehicles. Structural and morphological studies have been reported; cryo-TEM,<sup>1,2</sup> freeze-fracture electron microscopy,<sup>3</sup> synchrotron X-ray scattering,<sup>4–6</sup> and optical and fluorescence microscopy<sup>7,8</sup> have given a fairly good picture of the structure of these complexes as a function of the two most important parameters, lipid composition (e.g., type and quantity of the helper lipid, presence of cosurfactants) and charge ratio between the cationic lipid and DNA. The use of synchrotron radiation allowed the observation of the structures not only at higher concentrations (precipitates) but also in the dilute solutions (99% of water) used in gene therapy.<sup>4,5</sup> Recently, the enthalpies associated with the interaction between DNA and cationic vesicles were measured and found to be endothermic.<sup>9</sup> Thus, the driving force for the formation of the DNA–cationic vesicle complexes is entropic because of the release of counterions.

The purpose of the present work is to investigate the kinetic parameters that characterize the formation of DNA–cationic lipid complexes. A clear definition of the pathway and associated critical parameters is lacking. This lack can be partly ascribed to the complexity of the self-assembly process and the numerous parameters that contribute to the complex formation and structure.

Fluorescence spectroscopy is usually used as a method to follow stopped-flow reactions because of its inherent sensitivity and time resolution. Stopped-flow fluorometry seems to be a relevant technique to elucidate some of the aspects of DNA–cationic vesicle association through the use of extrinsic probes. The stopped-flow spectrofluorometric technique has been used to study the mechanism of intercalation into the DNA double helix by ethidium bromide,<sup>10</sup> as well as in the study of the interaction of proteins and phospholipid vesicles.<sup>11–13</sup> Ethidium

bromide (EB) is a well-known probe for DNA, and its ability to intercalate into the DNA double helix has been studied for several decades.<sup>14,15</sup> Ethidium bromide binds with little or no sequence preference at a stoichiometry of one dye per four to five base pairs of DNA. Its emission spectrum, quantum yields, and decay times are similar irrespective of the adjacent base pairs.<sup>16</sup> An activated process and not a diffusive process controls the intercalation of ethidium bromide into double-stranded DNA<sup>10</sup> because it is independent of the DNA chain length. Once intercalated between DNA base pairs, the ethidium ion does not form any bonds with the nucleotides but interacts with DNA through electrostatic, van der Waals, and hydrophobic forces. It distorts the sugar–phosphate backbone at the intercalation sites. Upon binding, its fluorescence is enhanced 20–30 times compared to the case of bulk water, the excitation maximum is shifted by ~30–40 nm to the red, and the emission maximum is shifted by ~15 nm to the blue. This makes this probe suitable for the study of the interaction of DNA with surfactants and drugs,<sup>17,18</sup> as well as the dynamics of DNA segments, and allows one to establish the state of the DNA by using gel electrophoresis.<sup>19</sup>

In this study, it is shown that the charge ratio (e.g., the relative concentrations of DNA and cationic vesicles) and variations in the composition of the lipid bilayer have a marked effect on the kinetics of interaction between DNA and cationic vesicles.

### Experimental Section

**Materials.** The zwitterionic lipid dioleoylphosphatidylethanolamine (DOPE) and the cationic lipid dioctadecyldimethylammonium bromide (DODAB) with purity higher than 99% as determined by HPLC were purchased from Avanti Polar Lipids (Alabaster, AL) and used without further purification. Salmon DNA (2000 bp as determined by 1% TAE agarose gel analysis, contour length 0.68  $\mu\text{m}$ ) was purchased from Gibco, BRL. The DNA concentration was measured by its absorbance at 260 nm,  $\epsilon = 6600 \text{ M}^{-1} \text{ cm}^{-1}$ . The ratio of the absorbance at 260 nm vs 280 nm was about 1.8–1.9, and the absorbance at

\* To whom correspondence should be addressed. E-mail address: Paula.Barreleiro@henkel.com. Present address: Paula Barreleiro, Henkel KGaA, Henkelstrasse 67, 40191 Düsseldorf, Germany.

320 nm was negligible, so no contamination of protein was observed. The conformation of DNA in aqueous solution was confirmed by circular dichroism (CD). The DNA melting temperature was measured by differential scanning calorimetry. A transition temperature of 49 °C was measured for DNA in 1 mM NaBr.

Unless specified otherwise, the concentrations of DNA solutions are given in moles of phosphate groups along the DNA backbone per cubic decimeter. Ethidium bromide (3,8-diamino-5-ethyl-6-phenylphenanthridium bromide, EB) was purchased from Boehringer-Mannheim and used without further purification. Ethidium bromide solutions are stable in pure distilled water kept in the dark at 4 °C. The concentrations of the stock solutions were evaluated from measurement of the absorbance at 480 nm using an extinction coefficient of 5700 M<sup>-1</sup> cm<sup>-1</sup>.

**Vesicle Preparation.** A lipid film was prepared by evaporation of chloroform under a N<sub>2</sub> stream from a chloroform solution of DODAB/DOPE at various molar ratios of DODAB/DOPE. The lipid film was placed overnight in a vacuum to remove the residual organic solvent. The film was then hydrated in water and then sonicated for 10 min (using a ultrasound bath) at 55 °C, which is above the gel-to-liquid-crystalline phase transition temperature (*T<sub>m</sub>*) of DODAB.<sup>20</sup> An extruder system (Avanti Polar Lipids, Alabaster, AL) was used to make vesicles of the desired size. Extrusion was performed at the same temperature through two stacked polycarbonate filters of pore size 400, 200, 100, and 50 nm. The size distribution of the liposome was determined by dynamic light scattering using a multiangle apparatus (Brookhaven Corporation Limited) equipped with a He–Ne laser (127 model, Spectra Physics,  $\lambda_0 = 632.8$  nm) with a 35 mW power. The scattered light was detected by a photomultiplier and analyzed with a 136 channel correlator (model BI2030AT). Samples were thermostated at 25 °C in a water bath. The number of counts in the autocorrelation decay was always higher than 10<sup>6</sup>. The solutions were centrifuged at 1300 g/h to remove dust.

**Lipoplex Preparation.** DNA and stock solutions of vesicles were diluted in water. Vesicle (or DNA) solutions were rapidly added to the DNA (or vesicle) solutions and mixed rapidly to prepare anionic (or cationic) complexes to achieve the desired charge ratio (defined as the ratio of positive charge equivalents of the cationic lipid component to negative charge equivalents of the nucleic acid component).<sup>21</sup> These studies were performed in distilled water (pH 5.5–6) at very low ionic strength (electrolyte introduced from the dilute DNA solution), so the electrostatic interactions to a large extent were unscreened.

**Stopped-Flow Spectroscopy.** *Fluorescence.* Static fluorescence measurements were performed in a SPEX Fluorolog. The excitation wavelength was set to 510 nm, at which the DNA-bound and free EB have the same molar extinction coefficient.<sup>22</sup> The fluorescence of the ethidium bromide is shifted to shorter wavelengths upon binding with DNA. Slits of excitation and emission of 1 mm were used, and the spectra were recorded from 525 to 700 nm. Upon condensation of the DNA helix, a decrease of the fluorescence intensity of the dye is observed. This decrease can arise from a change in the structure of the intercalating complex or from the exclusion of the ethidium bromide from the DNA molecule. Regardless the mechanism of fluorescence decrease it implies that a change in the DNA conformation has occurred and the signal can be used to follow the reaction of formation of DNA–cationic vesicle complexes.

The fluorescence kinetic recordings were obtained in a stopped-flow spectrofluorometer (Applied Photophysics SX.18MV SK.1E). The excitation monochromator was set to 510 nm, and

the emission monochromator was set to 590 nm as in the static measurements. The temperature was set to 25 °C. The dead time of the instrument was determined from the test reaction described elsewhere<sup>23</sup> and was estimated to 4 ms for a 1:1 mixing. Suitable control experiments were performed by mixing a solution of DNA and ethidium bromide and water (in the presence and absence of NaBr salt) or an ethidium bromide solution with cationic vesicle dispersions. Excitation of the EtBr/DNA complex may result in photobleaching of the dye and breaking of the double helix. Photobleaching of the dye was excluded because the signal of ethidium bromide intercalated into DNA when mixed with water was unchanged over the time of the measurement.

There can be orientation effects of DNA samples induced by the flow. To avoid degradation against shear gradients, one has to reduce the flow rate (e.g., decrease shear rate,  $\gamma$ , or Reynolds number, *Re*). However, the orientation effects cannot contribute to the measured signals for samples with rotational time constants much lower than 10 ms. The rotational time for 2900 bp DNA fragments is given to be 0.88 ms<sup>10</sup> (at 20 °C), so we can conclude that for the conditions of our experiments the orientation effects are not present.

*Turbidity.* The turbidity kinetic recordings were obtained in a stopped-flow spectrometer (Applied Photophysics SX.18MV.1E). The wavelength was set to 410 nm, and the temperature was 25 °C. The control experiments performed were the mixing of a lipid vesicle dispersion with water and a DNA solution with water and measuring the change in intensity as a function of time. In the control experiments, no change in intensity was observed; thus, the lipid vesicles were stable upon dilution.

**Data Treatment/Kinetic Analysis.** The observed kinetics is complex, clearly showing the presence of multiple steps. The kinetic analysis is based on the experimental time dependence of the fluorescence accompanying the binding of DNA to cationic vesicles. We assume that the fluorescence curves are a superposition of exponential terms:

$$I(t) = \sum_{i=1}^3 A_i \exp(-t/\tau_i) \quad (1)$$

where *I* is the fluorescence at time *t*, *A<sub>i</sub>* is the prefactor, and  $\tau_i$  is the pseudo-first-order time constant. The Nelder–Mead simplex method for minimizing eq 1 was applied. The quality of the fits was assessed from the  $\chi^2$  value.

**Circular Dichroism.** The circular dichroism (CD) spectrum in the vicinity of 260 nm is sensitive to the DNA helical structure. DNA in solution exhibited a spectrum with a peak at 273 nm, which is derived from the B-form of DNA.<sup>24</sup>

## Results

We performed stopped-flow fluorescence measurements to study the kinetics of the interaction between DNA and cationic vesicles. Ethidium bromide (EB) was used as the fluorescent probe. An aqueous solution of EB gives a weak fluorescence emission with a broad  $\lambda_{\text{max}}$  at ca. 590 nm when excited at 510 nm (Figure 1). When ethidium bromide intercalates into the DNA helix, the fluorescence emission increases by more than 1 order of magnitude (the “light-switch” mechanism).<sup>25</sup>

**Choice of EtBr/DNA Ratio.** As shown by Eastman et al.,<sup>26</sup> the decrease of EB fluorescence with increasing lipid concentration is dependent on the concentration of ethidium relative to DNA. Only if the ratio of EB to nucleotide is larger than one EB per six nucleotides is this decrease directly proportional to the amount of cationic lipid at a given DNA concentration. At

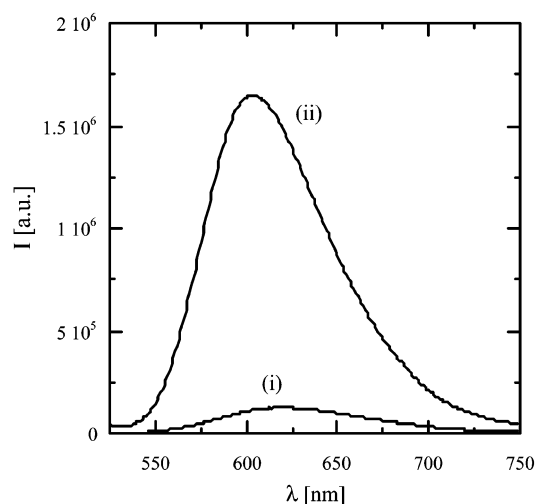


**Figure 1.** Ethidium bromide fluorescence spectrum: (i) absence of DNA; (ii) intercalated in DNA (0.075 mg/mL). Excitation wavelength was set at 510 nm.

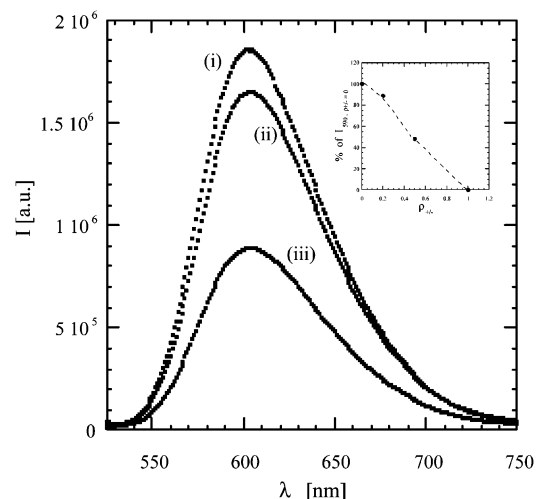


**Figure 2.** Ethidium bromide fluorescence spectra in the presence of mixed cationic vesicles at different charge ratios,  $\rho_{+/-}$ : (i) 0; (ii) 0.2; (iii) 0.5. The inset shows fluorescence intensity given as percentage (%) of the maximum (at 590 nm) as a function of charge ratio.

ratios of EB to nucleotide smaller than 1:6, the decrease in fluorescence had a sigmoidal profile<sup>27</sup> that can lead to erroneous interpretations. Thus, we used a ratio of one EB to five nucleotide units to obtain a linear decrease of the fluorescence. Figure 2 shows the decrease in fluorescence intensity of the dye in the presence of cationic vesicles. In the inset, the percentage of the intensity of the maximum (at 590 nm) corrected for the background fluorescence is given as a function of the charge ratio. We can see that the EB fluorescence is directly proportional to the amount of cationic lipid added at a constant amount of DNA. Please notice that the intensity at 590 nm has been corrected for the background fluorescence.

**DNA–Cationic Vesicle Complexation.** The formation of DNA–cationic vesicle complexes was followed by the decrease in fluorescence intensity after rapidly mixing DNA and cationic vesicle solutions of equal volumes. The decrease of the fluorescence can arise from the exclusion of the ethidium bromide from the DNA molecule or from a change in the structure of the intercalating complex. Regardless of the mechanism of the fluorescence decrease, it implies that a change of the DNA conformation has occurred and the signal can be used to follow the reaction of formation of DNA–cationic

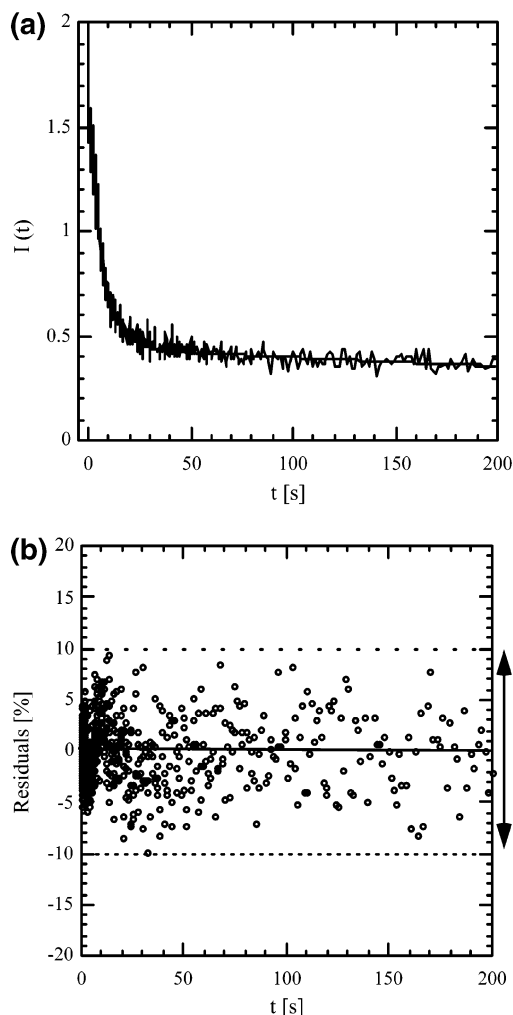


**Figure 3.** Stopped-flow recordings (a) corresponding to the fluorescence intensity (given as photomultiplier tube output voltages) decay of ethidium bromide observed upon addition of extruded cationic unilamellar vesicles to DNA at 25 °C. Initial concentration of DNA was 0.23 mM, and final charge ratio,  $\rho_{+/-}$ , was 1.5. The smooth line shows the fit. Panel b shows the residuals of the fit.

vesicle complexes. The quenching can be reversed when molecules that displace DNA from the complex are mixed with the cationic vesicle–DNA complex.<sup>28</sup>

A representative result from the stopped-flow experiments is shown in Figure 3a for the addition of DODAB/DOPE (1:1) to salmon DNA for a charge ratio,  $\rho_{+/-}$ , of 1.5. The kinetic curves show a multiexponential decay and were analyzed by fitting them to a sum of exponentials (eq 1). The number of exponentials was increased until no systematic deviation of the residual was found (Figure 3b). Three exponentials were necessary to fit the data.

**Effect of Charge Ratio on Kinetics.** Figure 4a shows experimental plots of the fluorescence intensity as a function of time and charge ratio for the reaction between DNA and DODAB/DOPE (1:1) 200 nm vesicles at constant DNA concentration at 25 °C. At this temperature, the vesicles are in the fluid state.<sup>9</sup>

Figure 4b shows the amplitudes calculated from Figure 4a as a function of charge ratio. A maximum for  $\rho_{+/-}$  as a function of charge ratio is observed. The fluorescence curves were fitted to eq 1. Table 1 shows the reciprocal of the time constants,  $\tau_1$ ,  $\tau_2$ , and  $\tau_3$  ( $k'_1$ ,  $k'_2$ , and  $k'_3$ ) as a function of the charge ratio,  $\rho_{+/-}$ , for DODAB/DOPE (1:1) 200 nm vesicles at constant DNA concentration and temperature. Each rate constant is the average

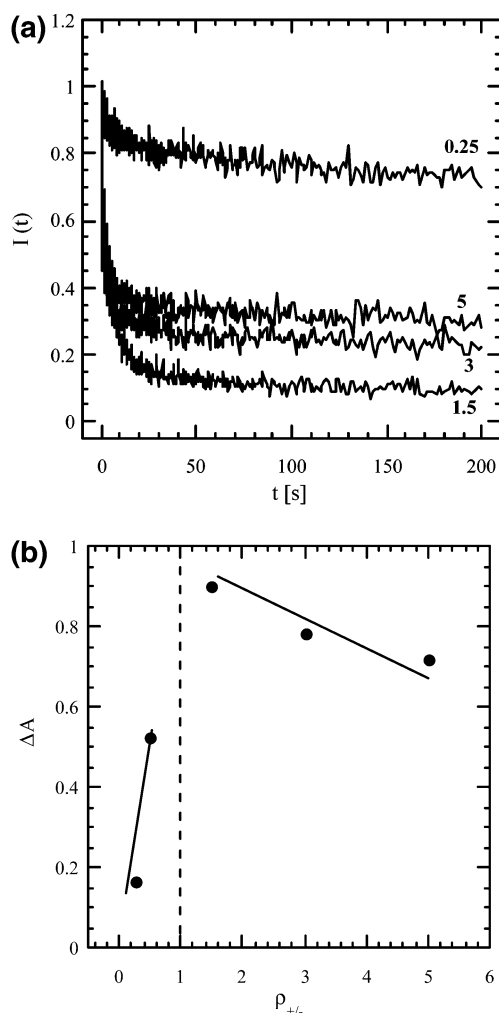


**Figure 4.** Fluorescence intensity (a) vs time for DNA binding to DODAB/DOPE (1:1) vesicles (200 nm) at various charge ratios. The charge ratios are indicated in the plot. Panel b shows the relative change of the fluorescence emission ( $\Delta A$ ) as a function of charge ratio.

**TABLE 1: Reciprocal of Time Constants for DNA Binding to DODAB/DOPE (1:1) Unilamellar Vesicles (200 nm) as a Function of the Charge Ratio,  $\rho_{+/-}$**

| charge ratio, $\rho_{+/-}$ | $k'_1$ ( $s^{-1}$ ) | $k'_2$ ( $s^{-1}$ ) | $k'_3$ ( $s^{-1}$ ) |
|----------------------------|---------------------|---------------------|---------------------|
| 0.25                       | $13.8 \pm 0.7$      | $0.08 \pm 0.02$     | $0.006 \pm 0.001$   |
| 0.75                       | $12.8 \pm 1.1$      | $0.17 \pm 0.03$     | $0.005 \pm 0.002$   |
| 1.5                        | $28.6 \pm 2.7$      | $0.14 \pm 0.02$     | $0.005 \pm 0.002$   |
| 3.0                        | $23.7 \pm 2.2$      | $0.49 \pm 0.05$     | $0.006 \pm 0.001$   |
| 5.0                        | $24.5 \pm 1.5$      | $0.64 \pm 0.06$     | $0.006 \pm 0.001$   |

of three independent experiments. The time constants are well separated; for example, for  $\rho_{+/-} = 1.5$ , we have  $\tau_2/\tau_1 \approx 200$  and  $\tau_3/\tau_2 \approx 30$ . The first apparent rate constant,  $k'_1$ , is fast and invariant with the charge ratio in the two regimes, that is, complexes with excess DNA ( $\rho_{+/-} < 1$ ) and complexes with excess lipid ( $\rho_{+/-} > 1$ ), and is higher for complexes with  $\rho_{+/-} > 1$ . The second rate constant,  $k'_2$ , increases with charge ratio. The third rate constant,  $k'_3$ , does not vary with charge ratio and has a constant value of around 600 s ( $k_3 = 0.0056 \pm 0.0024$   $s^{-1}$ ), which is consistent with the time obtained from time-resolved neutron scattering experiments.<sup>30,31</sup> We believe it stems from the rearrangement of the complex into multilamellar structures.

#### Effect of the Cationic Liposome Composition on Kinetics.

To determine whether the DOPE inclusion in the cationic vesicles is correlated with an alteration of the kinetics of the

**TABLE 2: Reciprocal of the Time Constants for DNA Binding to DODAB/DOPE Unilamellar Vesicles (200 nm),  $\rho_{+/-} = 3$ , as a Function of the Lipid Composition**

| $X_{\text{DODAB}}$ | $k'_1$ ( $s^{-1}$ ) | $k'_2$ ( $s^{-1}$ ) | $k'_3$ ( $s^{-1}$ ) |
|--------------------|---------------------|---------------------|---------------------|
| 0.33               | $27.6 \pm 2.5$      | $0.45 \pm 0.02$     | $0.007 \pm 0.001$   |
| 0.50               | $23.7 \pm 2.2$      | $0.49 \pm 0.05$     | $0.006 \pm 0.001$   |
| 0.67               | $16.5 \pm 1.3$      | $0.24 \pm 0.04$     | $0.007 \pm 0.002$   |
| 1.0                | $16.6 \pm 1.4$      | $0.13 \pm 0.03$     | $0.006 \pm 0.001$   |

interaction between DNA and vesicles, we investigated the reaction rates as a function of the lipid composition of the cationic vesicles. Pure DOPE does not form bilayers and liposomes at normal conditions because of its packing parameter but participates in a bilayer structure if stabilized by a bilayer-forming lipid such as DODAB. Cryo-TEM experiments (unpublished results, Barreleiro et al.) show that vesicles are formed with DODAB/DOPE mixtures for a mole fraction of DODAB above 0.25. In Table 2, the reciprocals of the time constants are given as a function of the molar fraction of the cationic lipid in the mixed cationic vesicle,  $X_{\text{DODAB}}$ . Each rate constant is the average of three independent experiments. The concentration of DODAB was kept constant, and the concentration of DOPE was varied. A decrease of  $k'_1$  and  $k'_2$  is observed with decreasing amounts of DOPE in the vesicles as shown in Table 2, while  $k'_3$  is roughly invariant. Pure DODAB bilayers are in the gel state at room temperature. Inclusion of DOPE in the DODAB cationic vesicle increases the bilayer fluidity<sup>9</sup> and reduces the surface charge density of the vesicles. For the compositions  $X_{\text{DODAB}} = 0.33$  and 0.5, different  $k'_1$  were obtained, while  $k'_2$  and  $k'_3$  were roughly the same. The vesicle bilayers are in the fluid phase at 25 °C; thus, the different  $k'_1$  obtained may be due to the different surface charge densities of the vesicles. The lipid vesicles with the compositions of  $X_{\text{DODAB}} = 0.67$  and 1 are in the gel state at room temperature. For these vesicles, different  $k'_2$  were obtained, while  $k'_1$  and  $k'_3$  were roughly the same. The lower values for  $k'_1$  and  $k'_2$  for vesicles in the gel state ( $X_{\text{DODAB}} = 0.67$  and 1), even though with higher surface charge density, suggest that cationic lipids with high melting temperatures are less responsive to DNA binding because in the gel state the cationic lipid bilayers may not be flexible enough for an efficient interaction with DNA. Circular dichroism measurements (see next section) also confirmed that DNA does not undergo a significant conformation change upon interaction with pure DODAB vesicles.

**Circular Dichroism Studies.** The effect of adding cationic vesicles on the helical structure of DNA was studied by recording the CD spectra of DNA upon adding mixed cationic vesicles (Figure 5). The CD spectrum of the pure DNA with a peak at 273 nm is characteristic of the B-form; it shows a long-wave positive and a short-wave negative band of roughly the same magnitude with an intersection point at about the absorption maxima.<sup>24</sup> Addition of pure DODAB vesicles has a minor effect on CD spectrum. Upon addition of vesicles in the fluid state, both the positive and the negative CD bands became gradually reduced. Also a red shift of the peak to 285 nm occurs. Thus, the CD spectrum becomes more similar to the C-form of DNA. The structural differences between the B-form and the C-form are such that the C-form has a larger winding angle and a smaller narrow groove.<sup>24</sup> An increase of the rotational angle and inclination probably makes intercalation of the ethidium bromide molecule to DNA weaker, and thus, the fluorescence emission intensity is reduced. Thus a change of the DNA conformation occurs as observed for other vesicle systems with the lipid bilayer in the fluid state.



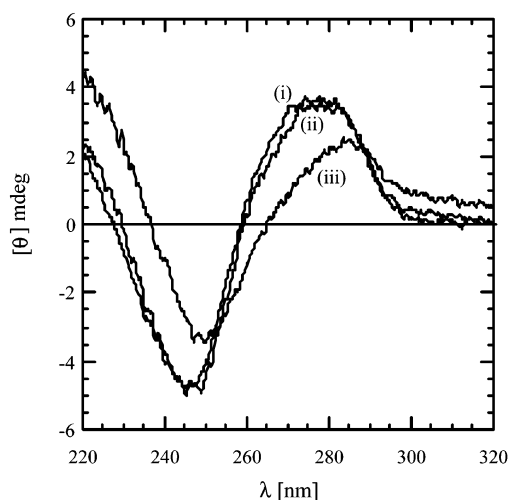


**Figure 5.** Circular dichroism studies showing effect of DODAB/DOPE vesicles on the CD spectrum of salmon DNA,  $\rho_{+/-} = 0.5$ : (i) salmon DNA in the absence of cationic vesicles; (ii)  $X_{\text{DODAB}} = 1$ ; (iii)  $X_{\text{DODAB}} = 0.5$ .

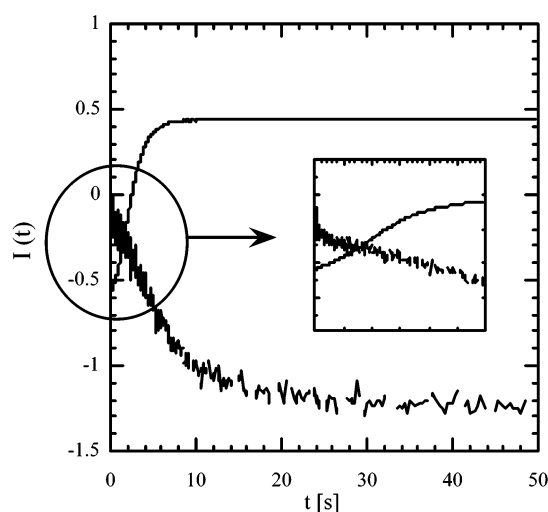


**Figure 6.** Comparison between fluorescence and turbidity data for DNA–DODAB/DOPE (1:1) complex with a charge ratio,  $\rho_{+/-}$ , of 1.5, a concentration of DNA of 0.23 mM, and an initial vesicle size of 200 nm.

**Comparison between the Fluorescence and Turbidity Data.** The fluorescence results describe the interaction between DNA and liposomes as seen from the perspective of the DNA. Changes in the size of the lipid aggregate can be probed with turbidity. Figure 6 shows the fluorescence and turbidity curves obtained after mixing DODAB/DOPE (1:1) vesicles and DNA with a charge ratio,  $\rho_{+/-}$ , of 1.5. We observe that the first time constant,  $\tau_1$ , is the same in both turbidity ( $k'_1 = 26.5 \pm 1.8 \text{ s}^{-1}$ ) and fluorescence measurements ( $k'_1 = 28.6 \pm 2.7 \text{ s}^{-1}$ ), while different rate constants were obtained for the second process:  $k'_2 = 0.14 \pm 0.02 \text{ s}^{-1}$  for fluorescence and  $k'_2 = 0.52 \pm 0.05 \text{ s}^{-1}$  for turbidity. The first time constant was assigned to the reaction of cationic vesicles with DNA with the formation of a larger particle (turbidity curve) and a change of the DNA conformation (fluorescence curve). The two curves confirm the existence of at least two processes. The second process is probably the formation of an unstable intermediate. No third step was observed in the turbidity measurements. Because no photobleach of the probe was observed over a period of 1000 s, the possibility of the third process being due to the photobleaching of the probe is excluded. We suggest a rear-

range of the complex associated with a change of the DNA conformation. The time scale of this third process is consistent with the appearance of a Bragg peak that we observed in time-resolved neutron scattering experiments performed in our group.<sup>30,31</sup>

## Discussion

We investigated the interaction between DNA and cationic vesicles using a stopped-flow fluorescence system. Although equilibrium studies appear frequently in the literature, only a few studies are reported concerning the kinetics and pathways of the transition under nonequilibrium conditions. An interesting study shows that the understanding of the pathways that lead to the final equilibrium and the plausible steps involved in the nonequilibrium states are important to produce dispersions of DNA complex of optimal size and composition. As pointed out by Bloomfield,<sup>32</sup> the size distribution of condensed particles may be determined by kinetic rather than thermodynamic factors. Also, the DNA–cationic vesicle complexes are prepared by a pipetting technique in which DNA (or cationic vesicles) are added into a tube containing cationic vesicles (or DNA). This preparation method does not allow the control of shear rate ( $\dot{\gamma}$ ) and Reynolds number ( $Re$ ) during the preparation of the complexes.<sup>33</sup> These parameters control the flow characteristics occurring during mixing and should be controlled within an optimal range.

The reaction was followed by a decrease of the fluorescence from the initial intensity to the equilibrium value ( $I_\infty$ ). The reaction followed first-order kinetics and appeared to occur in three steps. The reciprocal of the time constants followed the order  $k'_1 > k'_2 > k'_3$ . In the first step, the negatively charged phosphate groups of DNA interact with the cationic vesicle by electrostatic interactions and the ethidium bromide molecules are displaced into the solution. This process is fast and yields high  $k'_1$  values. A second step was observed with lower  $k'_2$  values. This subsequent release of ethidium bromide molecules to the solution may be due to formation of a cylindrical intermediate in which another cationic bilayer surrounds the DNA molecule as suggested by small-angle neutron scattering experiments.<sup>30,31</sup> These two steps make the secondary structure of DNA more compact, leading to a tertiary folding with exposure of more sites of DNA for binding with the cationic bilayer (and consequently release of even more ethidium bromide to solution), which yields a third time constant. A three-step process was also observed for the reaction of DNA with surfactants, such as cetyltrimethylammonium bromide (CTAB) and dodecyltrimethylammonium bromide (DTAB).<sup>34</sup> The third step seems to be due to the rearrangement of the complex and occurs on longer time scales ( $\sim 600 \text{ s}$ ). Different time constants were obtained when interacting DNA with cationic vesicles for different lipid compositions. Both  $k'_1$  and  $k'_2$  decreased with increasing  $X_{\text{DODAB}}$ . When changing the lipid composition, both the surface charge density and the lipid phase state are changed. However from Table 2, we can observe that the lipid phase state seems to be the main factor responsible for the observed changes in the rate constants. The fact that  $k'_3$  is invariant with the lipid composition suggests that once the DNA is intercalated between the lipid bilayers the release of the ethidium bromide molecules occurs at the same rate regardless of the state of the bilayer (phase and charge density). One has to notice that with fluorescence we are following the changes that occur from the DNA perspective. However, time-resolved neutron scattering studies performed in our group allow us to give a more complete picture of the mechanism of formation of DNA–cationic vesicle complexes.<sup>30,31</sup>

Other parameters such as lipid concentration, vesicle size, and preparation method may influence the kinetics of formation of DNA–cationic vesicle complexes. These variables were found to be important in the DNA-induced fusion of phosphatidylcholine vesicles.<sup>35</sup>

This proposed mechanism is also consistent with observations made by optical microscopy;<sup>36</sup> after a first injection of DNA into a vesicle solution, part of the membrane is destabilized and becomes highly fluctuating. An eruption of the vesicles toward the inner space is produced within 1 s. Further injections destabilize the membrane, and a series of endocytic vesicle eruptions follow with an interval of a few seconds, after which the internal vesicles go out of the giant unilamellar vesicle mimicking exocytosis. The initial vesicle reheals with a smaller diameter, and finally it is transformed into a multilayered lipid/DNA aggregate of irregular shape.

It is often believed that the complexation of DNA with cationic lipids is an irreversible reaction. However, it was shown that the addition of salt dissociates the DNA–cationic vesicle complex in accordance with the Manning theory.<sup>29</sup> Interacting the complex with anionic liposomes also showed the reversibility.<sup>28</sup> The reversibility is important for clinical reasons because the DNA must be released and this depends on the strength of the interaction and the reversibility of the interaction process. With this work, we hope to contribute to the understanding of the mechanisms behind the DNA–cationic vesicle complexation event, which would allow the production of more homogeneous, efficient delivery systems in pharmaceutically acceptable forms.

## Conclusion

Stopped-flow fluorescence can be used to monitor the kinetics of DNA–cationic vesicle complex formation. The binding followed first-order reactions and appeared to occur in three steps. The association reaction of DNA with cationic vesicles is complicated, and more than one exponential is required to fit the experimental curves. We believe that the complexity originates from the existence of many intermediate forms. Further investigations of the structure of the intermediates formed, involving time-resolved neutron scattering, are underway in our group.

**Acknowledgment.** We thank Daniel Otzen for providing access to stopped-flow apparatus. Support from the Swedish Natural Sciences Research Council (NFR) is acknowledged. P.C.A.B. also acknowledges the PRAXIS XXI, JNICT, for financial support, Scholarship BD/13788/97.

## References and Notes

- (1) Gustafsson, J.; Arvidson, G.; Karlsson, G.; Almgren, M. *Biochim. Biophys. Acta* **1995**, *1235*, 305.
- (2) Templeton, N. S.; Lasic, D. D.; Frederik, P. M.; Strey, H. H.; Roberts, D. D.; Pavlakis, G. N. *Nat. Biotechnol.* **1997**, *15*, 647.
- (3) Sternberg, B. J. *Liposome Res.* **1996**, *6*, 515.
- (4) Rädler, J.; Koltover, I.; Salditt, T.; Safinya, C. *Science* **1997**, *275*, 810.
- (5) Koltover, I.; Salditt, T.; Rädler, J. O.; Safinya, C. R. *Science* **1998**, *281*, 78.
- (6) Lasic, D. D.; Strey, H.; Stuart, M.; Podgornik, R.; Frederik, P. J. *Am. Chem. Soc.* **1997**, *119*, 832.
- (7) Koltover, I.; Rädler, J. O.; Safinya, C. R. *Phys. Rev. Lett.* **1999**, *82*, 1991.
- (8) Maier, B.; Rädler, J. O. *Phys. Rev. Lett.* **1999**, *82*, 1911.
- (9) Barreleiro, P. C. A.; Olofsson, G.; Alexandridis, P. *J. Phys. Chem. B* **2000**, *104*, 7795.
- (10) Stellwagen, N. C. *J. Biomol. Struct. Dyn.* **1985**, *3*, 299.
- (11) Bradrick, T. D.; Philippidis, A.; Georgiou, S. *Biophys. J.* **1995**, *69*, 1999.
- (12) Subramanian, M.; Jutila, A.; Kinnunen, P. K. *J. Biochemistry* **1998**, *37*, 1394.
- (13) Söderlund, T.; Jutila, A.; Kinnunen, P. K. *J. Biophys. J.* **1999**, *76*, 896.
- (14) Le Pecq, J. B.; Paoletti, C. *J. Mol. Biol.* **1967**, *27*, 87.
- (15) Waring, M. J. *J. Mol. Biol.* **1965**, *13*, 269.
- (16) Malak, H.; Castellano, F. N.; Grycznski, I.; Lakowicz, J. R. *Biophys. Chem.* **1997**, *67*, 35.
- (17) Medina, M. A.; Ramirez, F. J.; Ruiz-Chica, J.; Chavarria, T.; Lopez-Navarrete, J. T.; Sanchez-Jimenez, F. *Biochim. Biophys. Acta* **1997**, *1379*, 129.
- (18) Bhattacharya, S.; Mandal, S. S. *Biochim. Biophys. Acta* **1997**, *1323*, 29.
- (19) Åkerman, B. *Biophys. J.* **1998**, *74*, 3140.
- (20) Feitosa, E.; Barreleiro, P. C. A.; Olofsson, G. *Chem. Phys. Lipids* **2000**, *105*, 201.
- (21) Felgner, P. L.; Barenholz, Y.; Behr, J. P.; Cheng, S. H.; Cullis, L.; Huang, L.; Jessee, J. A.; Seymour, L.; Szoka, F.; Thierry, A. R.; Wagner, E.; Wu, G. *Hum. Gene Ther.* **1997**, *8*, 511.
- (22) Dufourcq, J.; Neri, W.; Henry-Toulme, N. *FEBS Lett.* **1998**, *421*, 7.
- (23) Tonomura, B.; Nakatani, H.; Ohnishi, M.; Yamaguchi-Ito, J.; Hiromi, K. *Anal. Biochem.* **1978**, *17*, 370.
- (24) Ivanov, V. I.; Minchenkova, L. E.; Schyolkina, A. K.; Poletayev, A. I. *Biopolymers* **1973**, *12*, 89.
- (25) Le Pecq, J. B. *Methods Biochem. Anal.* **1971**, *20*, 41.
- (26) Eastman, S. J.; Siegel, C.; Touseignant, J.; Smith, A. E.; Cheng, S. H.; Scheule, R. K. *Biochim. Biophys. Acta* **1997**, *1325*, 41.
- (27) Gershon, H.; Ghirlando, R.; Guttman, S. B.; Minsky, A. *Biochemistry* **1993**, *32*, 7143.
- (28) Xu, Y.; Szoka, F. J. *Biochemistry* **1996**, *35*, 5616.
- (29) Lasic, D. D. *Liposomes in gene therapy*; CRC Press LLC: New York, 1997.
- (30) Barreleiro, P. C. A.; Le, T.; May, R. P.; Lindman, B. *ILL Ann. Rep.* **2000**, 54.
- (31) Barreleiro, P. C. A.; May, R. P.; Lindman, B. *Faraday Discuss.* **2003**, *122*, 191–201.
- (32) Bloomfield, V. A. *Biopolymers* **1991**, *21*, 1471.
- (33) Hirota, S.; de Ilarduya, C. T.; Barron, L. G.; Szoka, J., F. C. *Biotechniques* **1999**, *27*, 286.
- (34) Maulik, S.; Jana, P. K.; Moulik, S. P.; Chattoraj, D. K. *Biopolymers* **1995**, *35*, 533.
- (35) Hayes, M. E.; Gorelov, A. V.; Dawson, K. A. *Prog. Colloid Polym. Sci.* **2001**, *118*, 243.
- (36) Angelova, M. I.; Hristova, N.; Tsoneva, I. *Eur. Biophys. J.* **1999**, *28*, 142.